Blood-Brain Barrier Permeable 2-Phenylbenzothiazolyl Iridium Complexes as Inhibitors and Probes of Aβ Aggregation

Yiran Huang,[†,#] Hanah Na,[†,#] Liang Sun,[†,#] Karna Terpstra,[†] Kai Gui,[†] Zhengxin Yu,[†] and Liviu M. Mirica[†,*]

[†]Department of Chemistry, University of Illinois at Urbana-Champaign, 600 S. Mathews Avenue, Urbana, Illinois 61801, United States

KEYWORDS: Alzheimer's disease; amyloid-β; iridium complexes; inhibition; BBB permeability

ABSTRACT: The aggregation of amyloid β (Aβ) peptides is a significant hallmark of Alzheimer's Disease (AD) and the inhibition and detection of Aβ aggregates are important for the treatment and diagnosis of AD. Herein, a series of benzothiazole-based luminescent Ir(III) complexes **HN-1** to **HN-8** were reported, which exhibit appreciable Aβ aggregation inhibition ability *in vitro* and in living cells. In addition, they are capable of inducing a fluorescence turn-on effect when binding to Aβ fibrils and oligomers. Most importantly, compared to previously reported cationic metal complexes, the neutral Ir complexes reported here show optimal Log D values, which suggest these compounds should have enhanced blood brain barrier (BBB) permeability. Most importantly, *in vivo* studies show that the neutral Ir complexes **HN-2**, **HN-3**, and **HN-8** successfully penetrate the BBB and stain amyloid plaques in AD mice brains after a 10-day treatment via i.p. injection, which is unprecedented for Ir(III) complexes, and thus can be used as lead compounds for AD therapeutics development.

INTRODUCTION

Alzheimer's disease (AD) is the most common neurodegenerative disease and the 6th cause of death in the US.[1] One of the strategies for the treatment of AD is the development of inhibitors that prevent the misfolding and self-assembling aggregation of monomeric Aβ peptides into neurotoxic Aβ species.[2-8]

Transition metal complexes have emerged as a viable alternative to organic compounds with distinct biological properties and have been wildly utilized for the treatment of cancer.[9-10] Recently, transition metal complexes have been developed as chemical reagents capable of altering Aβ aggregation.[11-25] Among many of these transition metal complexes, cyclometalated Ir(III) complexes would be one of the most promising candidates as their photophysical and photochemical properties are unique and desirable. In general, these complexes exhibit high luminescence quantum yields and long lifetimes due to the efficient spin-orbit coupling induced by the heavy Ir(III) center. Also, they have high thermal and chemical stability, as Ir(III) is a substitutionally inert transition metal ion.[26-27] Not only that, tuning the emission color and excited-state dynamics is easily achieved through ligand structure modification, by either increasing conjugation, introducing heteroatoms, and/or various substituents. Furthermore, the preparation of Ir(III) complexes is highly modular compared to the multistep and linear syntheses of organic molecules. Thus, cyclometalated Ir(III) complexes can usually be prepared in fewer steps and with greater flexibility for modification during the synthesis of each module.[28-29] This synthetic versatility could be exploited to enhance the interaction of Ir(III) complexes with Aβ species, which could leads to the consequent modulation of the Aβ aggregation pathways.

In this work, eight Ir(III) complexes were designed and synthesized with the incorporation of Aβ binding parts as ligands. These complexes with two or three Aβ binding groups are stable and exhibit optimsl log D values and appreciable affinity for Aβ fibrils and oligomers. Furthermore, we demonstrate that in *in vivo* studies, three of the Ir(III) complexes show the ability to cross the blood brain barrier (BBB) and specifically label the amyloid species in the brains of transgenic AD mice.

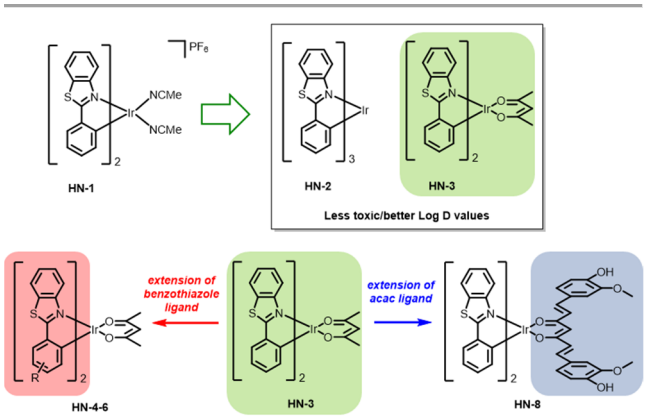

Figure 1. Rational design strategies of Ir(III) Complexes

RESULTS AND DISCUSSION

Design, Synthesis and Characterization of Ir(III) Complexes. Complexes **HN-1-3**, with 2-phenyl-1,3-benzothiazole molecules as C^N ligands, were first designed and synthesized as the starting point for the subsequent studies.

HN-1 is a cationic Ir(III) complex with two labile acetonitrile (MeCN) ancillary ligands, which allows for potential coordination to the Aβ amino acid residues. Then, **HN-2** was designed as a neutral tris-Ir(III) complex with the idea of increasing lipophilicity and the potential to penetrate blood brain barrier (BBB). **HN-3** was also a neutral complex with an acetylacetonate (acac) ancillary ligand, which could be further modified or elongated. Complexes **HN-4-6** were constructed by extension of the 2-phenyl-1,3-benzothiazole C^N ligand with a pendant free-rotating moiety. We proposed that the pendant moiety could rotate freely in the solution but get rigidified when Ir(III) complexes bind to fibrils, and this would achieve the fluorescence "switch-on" effects as Aβ probes. Complex **HN-8** was designed by replacing the acac ligand with curcumin (a natural product which has been reported to have the ability to alleviate Aβ toxicity),[30-32] and its synthesis is more practical and easy-to-achieve, since attaching the acac ligand is the last step in the development of these inert Ir(III) complexes.

The molecular structure of **HN-1** was determined by single-crystal X-ray diffraction and is shown in Figure 2. The Ir atom adopts a distorted octahedral coordination geometry, with two C^N cyclometalated ligands and two acetonitrile ligands. The C^N nitrogen atoms are in a *trans* orientation relative to each other. The Ir–C and Ir–N (C^N) bond lengths of **HN-1** are similar to those of the previously reported Ir(III) complexes with 2-phenyl-1,3-benzothiazole C^N ligand, ranging 2.007–2.143 Å.[29, 33-34]

Scheme 1. Synthetic routes to Ir(III) complexes. (a) Complexes HN-1-7; (b) complex HN-8.

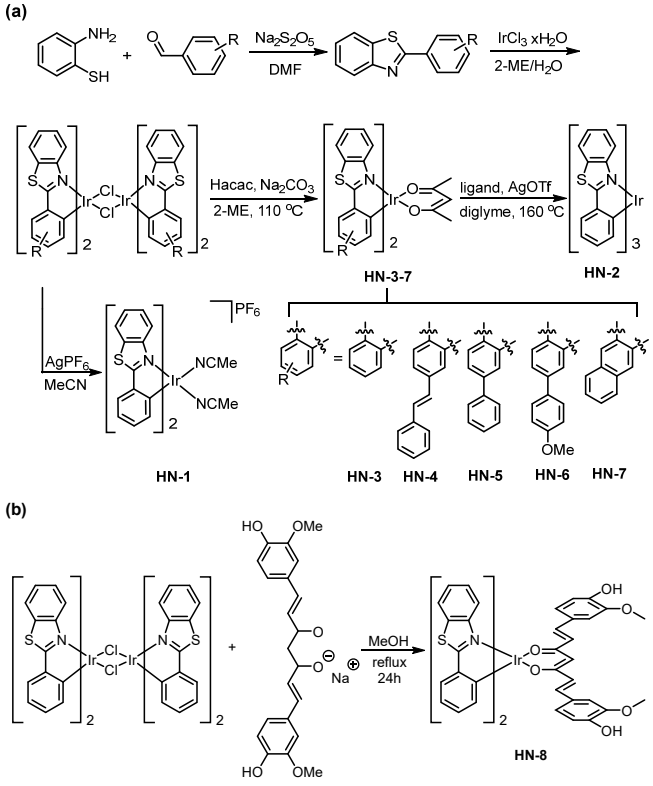

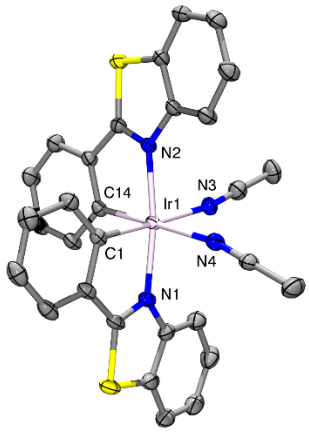

Figure 2. X-ray crystal structure of **HN-1**. Thermal ellipsoids are drawn at the 50% probability with solvent molecules, counter ion and hydrogen atoms are eliminated for clarity. Selected bond distances (Å): Ir1–C1, 2.007(3); Ir1–C14, 2.008(3); Ir1–N1, 2.061(3); Ir1–N2, 2.064(3); Ir1–N3, 2.128(3); Ir1–N4, 2.143(3).

Photophysical and Biochemical Properties of Ir(III) Complexes. The UV-vis absorption spectra of **HN-1-8** were obtained in PBS with 0.5% DMSO (Figure S1). Complexes **HN-1-3** displayed intense absorption bands around 320 nm which can be assigned to spin-allowed ligand centered π–π* transitions (^{1}LC) and less intense charge transfer (^{1,3}CT) absorption bands tailing out to 500 nm. These complexes exhibit emission in the region of 520–700 nm (Figures 3a and Figure S2) in PBS with DMSO (<5%) where the Stokes shift is significantly large due to the phosphorescent properties of Ir(III) complexes.

As shown in Figure 3a (black line), **HN-1** showed an excellent turn-on response toward $Aβ_{42}$ fibrils. It displayed a 183-fold fluorescence intensity increase ($λ_{em}$ = 550 nm) for $Aβ_{42}$ fibrils, with a K_d value of 32.1 ± 9.1 μM (Figure S4). This is likely due to the MeCN ligands in the Ir(III) complex being replaced by amino acid residues of the Aβ aggregates and therefore the Ir(III) complex coordinates to the peptides, as proposed previously.[35-36]

In recent years, mounting evidence indicates that soluble Aβ oligomers are highly toxic for neurons.[37-38] Therefore, Ir(III) complexes developed in this study were also tested to see whether they could interact with soluble $Aβ_{42}$ oligomers. $Aβ_{42}$ oligomers were prepared according to the procedure reported by Klein and the morphology of obtained species was confirmed by transmission electron microscopy (TEM, Figure S3). Surprisingly, **HN-1** also showed a 142-fold fluorescence intensity increase with soluble $Aβ_{42}$ oligomers (Figure 3a, blue line) and its K_d value of oligomers is 25.1 ± 8.9 μM (Figure S4).

Complexes **HN-2** (Figure 3b) and **HN-3** did not exhibit apparent fluorescence increase when they bind to Aβ aggregates. This is also consistent with our previous assumption that the molecular structures of these complexes are too rigid. As expected, extended conjugated complexes **HN-4** and **HN-8** showed "turn-on" effects when they bind to Aβ fibrils, with a "15-fold" fluorescence increase for **HN-4**, and a "20-fold" increase for **HN-8**, respectively. The K_d values of

fibrils and oligomers of **HN-8** are 1.61 ± 0.46 μM and 3.46 ± 1.32 μM, respectively (Figure S4).

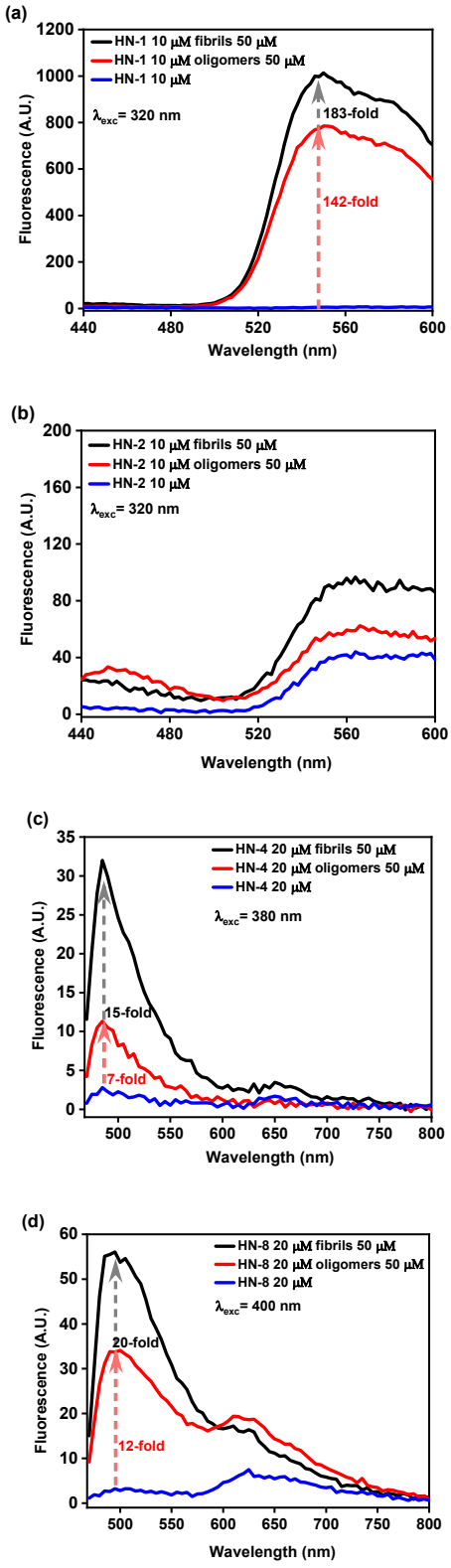

Figure 3. Fluorescence spectra of Ir(III) complexes with/without $A\beta_{42}$ fibrils or $A\beta_{42}$ oligomers. (a) **HN-1**, (b) **HN-2**, (c) **HN-4**, and (d) **HN-8**.

Inhibition of Amyloid β Aggregation. The Aβ inhibition abilities of the Ir(III) complexes were measured by performing thioflavin T (ThT) fluorescence assays. ThT is a well-established fluorophore for the kinetic measurement of Aβ aggregation, and it is known that when it binds to amyloid fibrils, a pronounced enhancement of fluorescence can be detected at λ_{max} = 485 nm upon excitation at 435 nm. The aggregation of Aβ occurs via a sigmoidal route, which is composed of three phases: lag phase, elongation phase, and a plateau phase (Figure 4, black line).

Compared to the control group, all Ir(III) complexes exhibit the ability to inhibit Aβ aggregation (stop or delay the aggregation). For **HN-1**, it completely quenched the Aβ aggregation (Figure 4, red line, inhibition percentage: 100%), probably due to the replacement of acetonitrile ligands of **HN-1** with histidine residue locating on the N-terminus of Aβ peptide, which plays critical role in Aβ aggregation.[39] Though the curcumin-Ir(III) complex **HN-8** accelerated the aggregation process at the beginning of the elongation phase, further progress was suppressed and accordingly, around 75% of a final inhibition percentage was obtained (Figure 4, orange line). This is consistent with the previous observation where curcumin derivatives can significantly inhibit the Aβ aggregation process.[31] All other Ir(III) complexes extended the lag phase and delayed the beginning of the elongation phase. We note that neither the excitation nor emission wavelength range of ThT overlaps with those of Ir(III) complexes.

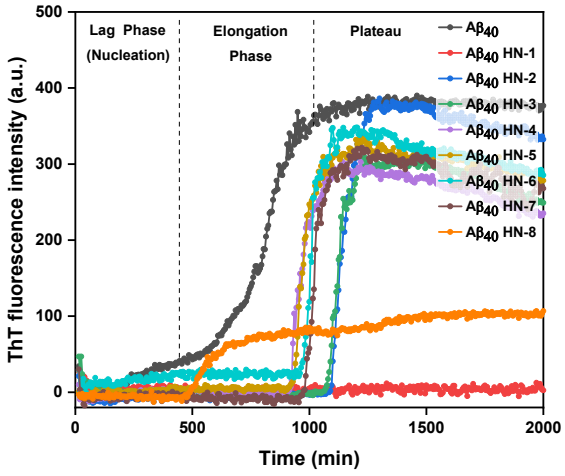

Figure 4. Time-resolved measurements of the aggregation of $A\beta_{40}$ through examination of ThT emission at 485 nm (λ_{ex} = 435 nm) for free $A\beta_{40}$ and $A\beta_{40}$ incubated with the ligands **HN 1-8**. Conditions: [$A\beta_{40}$] = 10 μM; [ThT] = 10 μM; [compound] = 10 μM.

5xFAD Mouse Brain Section Imaging. To examine whether those Ir(III) complexes could specifically interact with native Aβ species, brain section staining was performed. All brain sections were sliced from transgenic 5xFAD mice, which can overexpress human APP and PSEN1 transgenes. All of the eight Ir(III) complexes can specifically label Aβ plaques, showing excellent colocalization with

staining of CF594 conjugated HJ3.4 antibody (CF594-HJ3.4) that binds to a wide range of Aβ species.[40]

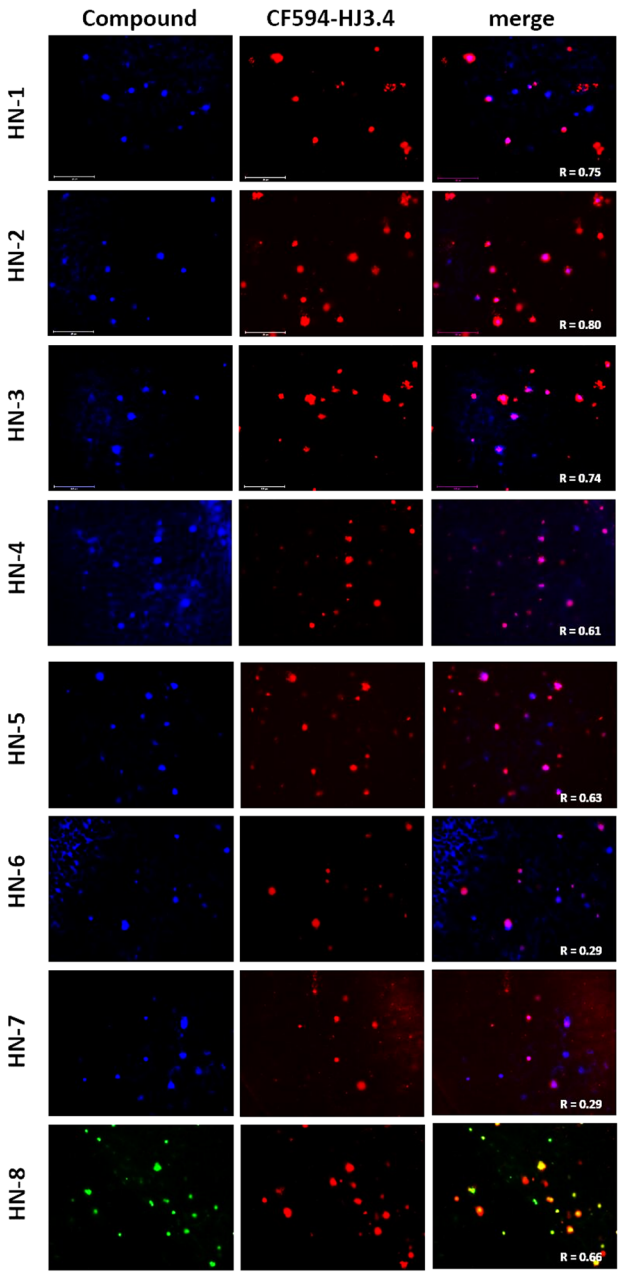

Figure 5. Fluorescence microscopy images of 5xFAD mice brain sections incubated with Ir(III) complexes. The fluorescence signals from Ir(III) complexes and CF594-HJ3.4 antibody were monitored under blue and red channels, respectively. Scale bar: 125 μm. R equals to Pearson's correlation coefficient.

LogD Measurements of Ir(III) Complexes. Log D values were also examined to evaluate the BBB permeability of the Ir(III) complexes. For complexes **HN-2-5, HN-7** and **HN-8**, they all showed Log D values in the range of 0.9–2.5, suggesting these compounds are promising candidates for further *in vivo* studies. In the case of **HN-1**, a cationic complex, it shows a lower Log D value due to charges. **HN-6** also showed low Log D value, presumably because of hydrogen bond formation through a methoxy group on the ligand of Ir(III) complex.

Table 1. Distribution coefficients(Log D) of Ir(III) complexes in octanol/PBS (pH 7.4).

Iridium complex	Log D
HN-1	0.650 ± 0.110
HN-2	1.220 ± 0.055
HN-3	1.313 ± 0.067
HN-4	1.013 ± 0.084
HN-5	1.113 ± 0.029
HN-6	0.571 ± 0.028
HN-7	1.509 ± 0.020
HN-8	1.434 ± 0.047

Cytotoxicity of Aβ Species upon Incubation with Ir(III) Complexes. The neurotoxicity of the Ir(III) complexes and their ability to alleviate the Aβ-induced neurotoxicity was investigated using mouse neuroblastoma (N2a) cells. First, we examined the toxicity of all Ir(III) complexes at various concentrations ranging from 2 to 20 μM (Figure 6a). Except for **HN-1**, all other iridium(III) complexes show very low cytotoxicity up to 20 μM.

Then, N2a cells were treated with $A\beta_{42}$ in the absence or presence of the Ir(III) complexes to investigate whether the inhibition of amyloid can result in the rescue of $A\beta_{42}$ neurotoxicity (Figure 6b). 20 μM of Aβ on its own is toxic to the cells. Co-treatment with all of the eight Ir(III) complexes showed significant rescues of Aβ-induced neurotoxicity. For comparison, the N2a cells were also treated with $A\beta_{42}$ with the presence of curcumin. The treatment of curcumin dramatically increased the Aβ-induced cytotoxicity, instead of rescuing the cells (Figure S5). Since curcumins are quite unstable in PBS and cell media, the metabolites may deteriorate the Aβ-mediated cytotoxicity. However, in case of the curcumin-Ir(III) complex **HN-8**, the chelation between the metal center and the ligand could stabilize the entire curcumin structure, thus resulting in improved cell viability. Overall, the cell data revealed that Ir(III) complexes developed in this work could efficiently decrease the Aβ-induced cytotoxicity for N2a cells and also be potential candidates for *in vivo* studies.

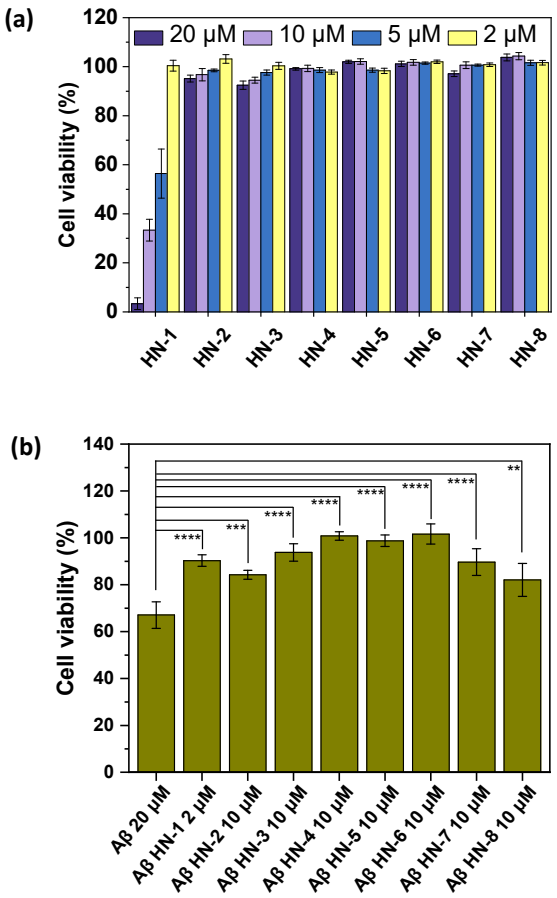

Figure 6. (a) Cytotoxicity studies of Ir(III) complexes. (b) Cytotoxicity studies of Ir(III) complexes with $A\beta_{42}$.

***In vivo* Blood-Brain Barrier Permeability.** The BBB permeability of the metal complexes has significant implications for *in vivo* applications in AD research. Until now, very few metal complexes have shown the ability to cross the BBB.[18] To evaluate the BBB permeability of investigated Ir(III) complexes, we administered three of the Ir(III) complexes **HN-2**, **HN-3,** and **HN-8** daily to 11-month old 5xFAD mice (1 mg/kg of body weight) via intraperitoneal injection for 10 days. All of three complexes show fluorescent staining signals in both DAPI and FITC channels (Figure S6). The fluorescence images demonstrated that the developed Ir(III) complexes could successfully penetrate the BBB, and the *in vivo* accumulated Ir(III) complexes have significant colocalizations with the amyloid species co-stained with HJ3.4 antibody (Figure 7). Overall, the immunofluorescence staining studies suggest that the developed Ir(III) complexes have the ability to cross the BBB and specifically label the amyloid species *in vivo*.

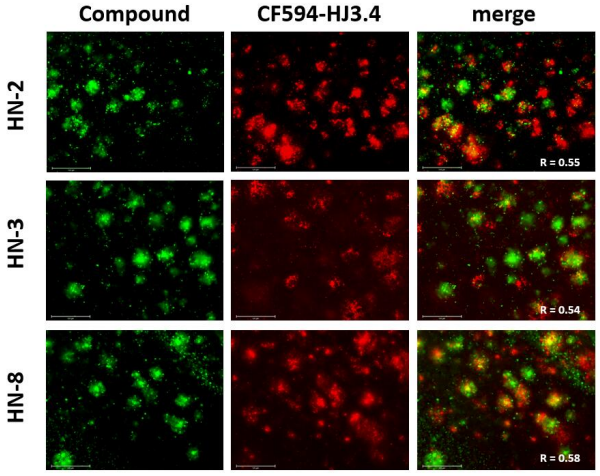

Figure 7. Representative fluorescence microscopy images of brain sections from 11-month old 5xFAD mice administrated with Ir(III) complexes for 10 days. The brain sections were co-immunostained with the HJ3.4 antibody ([HJ3.4] = 1 μg/ml, scale bar = 125 μm).

CONCLUSION

In this paper, a series of inert Ir(III) complexes were designed and synthesized, and they exhibit remarkable Aβ labeling and aggregation inhibition properties, and thus are promising to be used as probes and inhibitors for Aβ aggregation. The screening experiments revealed that complex **HN-8** shows excellent performance both in inhibiting Aβ species *in vitro* and alleviating the Aβ-induced cytotoxicity in living cells. In addition, compared to the other previous reported Ir(III) complexes, its hydrophobicity appreciable and holds significant promise to be used *in vivo*. Moreover, we have demonstrated that the rational design strategy via a simple extension of the benzothiazole framework or replacement of the acac ligand offers a practical way to develop Ir(III) complexes with optimal drug-like characteristics. Further studies will be performed on the modification of the different types of ligands, which allow Ir(III) complexes to emit in the near-infrared (NIR) region and thus can be employed in NIR imaging applications.

ASSOCIATED CONTENT

Supporting Information. Detailed synthetic procedures, UV-vis and emission spectra, and NMR spectra of Ir(III) Complexes.

AUTHOR INFORMATION

Corresponding Author

* mirica@illinois.edu

Author Contributions

#Y.H., H.N., and L.S. contributed equally to this work.

ORCID

Liviu Mirica: 0000-0003-0584-9508
Yiran Huang: 0000-0003-1755-9874
Hanah Na: 0000-0002-0576-4806

Liang Sun: 0000-0002-0080-0855

Notes

The authors declare no competing financial interest.

ACKNOWLEDGMENTS

L.M.M. acknowledges research funding from the NIH (R01GM114588).

REFERENCES

(1) *Alzheimer's & Dementia* **2020**, *16*, 391.
(2) Cho, H.-J.; Sharma, A. K.; Zhang, Y.; Gross, M. L.; Mirica, L. M. *ACS Chem. Neurosci.* **2020**, *11*, 1471.
(3) Savelieff, M. G.; Nam, G.; Kang, J.; Lee, H. J.; Lee, M.; Lim, M. H. *Chem. Rev.* **2019**, *119*, 1221.
(4) Huang, Y. R.; Cho, H. J.; Bandara, N.; Sun, L.; Tran, D.; Rogers, B. E.; Mirica, L. M. *Chem. Sci.* **2020**, *11*, 7789.
(5) Gomes, L. M. F.; Mahammed, A.; Prosser, K. E.; Smith, J. R.; Silverman, M. A.; Walsby, C. J.; Gross, Z.; Storr, T. *Chem. Sci.* **2019**, *10*, 1634.
(6) Ayala, S.; Genevaux, P.; Hureau, C.; Faller, P. *ACS Chem. Neurosci.* **2019**, *10*, 3366.
(7) Rodríguez-Rodríguez, C.; Telpoukhovskaia, M.; Orvig, C. *Coord. Chem. Rev.* **2012**, *256*, 2308.
(8) Bieschke, J.; Russ, J.; Friedrich, R. P.; Ehrnhoefer, D. E.; Wobst, H.; Neugebauer, K.; Wanker, E. E. *Proc Natl Acad Sci U S A* **2010**, *107*, 7710.
(9) Ho, P. Y.; Ho, C. L.; Wong, W. Y. *Coord. Chem. Rev.* **2020**, *413*.
(10) Szczepaniak, A.; Fichna, J. *Biomolecules* **2019**, *9*.
(11) Kang, J.; Nam, J. S.; Lee, H. J.; Nam, G.; Rhee, H. W.; Kwon, T. H.; Lim, M. H. *Chem. Sci.* **2019**, *10*, 6855.
(12) Suh, J. M.; Kim, G.; Kang, J.; Lim, M. H. *Inorg. Chem.* **2019**, *58*, 8.
(13) Man, B. Y.-W.; Chan, H.-M.; Leung, C.-H.; Chan, D. S.-H.; Bai, L.-P.; Jiang, Z.-H.; Li, H.-W.; Ma, D.-L. *Chem. Sci.* **2011**, *2*, 917.
(14) Kang, J.; Lee, S. J. C.; Nam, J. S.; Lee, H. J.; Kang, M. G.; Korshavn, K. J.; Kim, H. T.; Cho, J.; Ramamoorthy, A.; Rhee, H. W.; Kwon, T. H.; Lim, M. H. *Chem. Eur. J.* **2017**, *23*, 1645.
(15) Yellol, G. S.; Yellol, J. G.; Kenche, V. B.; Liu, X. M.; Barnham, K. J.; Donaire, A.; Janiak, C.; Ruiz, J. *Inorg. Chem.* **2015**, *54*, 470.
(16) Lu, L. H.; Zhong, H. J.; Wang, M. D.; Ho, S. L.; Li, H. W.; Leung, C. H.; Ma, D. L. *Sci. Rep.* **2015**, *5*.
(17) Hayne, D. J.; Lim, S.; Donnelly, P. S. *Chem. Soc. Rev.* **2014**, *43*, 6701.
(18) Kenche, V. B.; Hung, L. W.; Perez, K.; Volitakes, I.; Ciccotosto, G.; Kwok, J.; Critch, N.; Sherratt, N.; Cortes, M.; Lal, V.; Masters, C. L.; Murakami, K.; Cappai, R.; Adlard, P. A.; Barnham, K. J. *Angew. Chem., Int. Ed.* **2013**, *52*, 3374.
(19) Son, G.; Lee, B. I.; Chung, Y. J.; Park, C. B. *Acta Biomater* **2018**, *67*, 147.
(20) Derrick, J. S.; Lee, J.; Lee, S. J. C.; Kim, Y.; Nam, E.; Tak, H.; Kang, J.; Lee, M.; Kim, S. H.; Park, K.; Cho, J.; Lim, M. H. *J. Am. Chem. Soc.* **2017**, *139*, 2234.
(21) Wang, X. H.; Wang, X. Y.; Zhang, C. L.; Jiao, Y.; Guo, Z. J. *Chem. Sci.* **2012**, *3*, 1304.
(22) Kumar, A.; Moody, L.; Olaivar, J. F.; Lewis, N. A.; Khade, R. L.; Holder, A. A.; Zhang, Y.; Rangachari, V. *ACS Chem. Neurosci.* **2010**, *1*, 691.
(23) Aliyan, A.; Paul, T. J.; Jiang, B.; Pennington, C.; Sharma, G.; Prabhakar, R.; Martí, A. A. *Chem* **2017**, *3*, 898.
(24) Barnham, K. J.; Kenche, V. B.; Ciccotosto, G. D.; Smith, D. P.; Tew, D. J.; Liu, X.; Perez, K.; Cranston, G. A.; Johanssen, T. J.; Volitakis, I.; Bush, A. I.; Masters, C. L.; White, A. R.; Smith, J. P.; Cherny, R. A.; Cappai, R. *Proc. Natl. Acad. Sci. U. S. A.* **2008**, *105*, 6813.
(25) Suh, J.; Yoo, S.; Kim, M.; Jeong, K.; Ahn, J. Y.; Kim, M. S.; Chae, P. S.; Lee, T. Y.; Lee, J.; Lee, J.; Jang, Y. A.; Ko, E. H. *Angew. Chem., Int. Ed.* **2007**, *46*, 7064.
(26) Lowry, M. S.; Bernhard, S. *Chem. Eur. J.* **2006**, *12*, 7970.
(27) Helm, L.; Merbach, A. E. *Chem. Rev.* **2005**, *105*, 1923.
(28) Zhou, Y. Y.; Gao, H. F.; Wang, X. M.; Qi, H. L. *Inorg. Chem.* **2015**, *54*, 1446.
(29) Wang, R. J.; Liu, D.; Ren, H. C.; Zhang, T.; Wang, X. Z.; Li, J. Y. *J. Mater. Chem.* **2011**, *21*, 15494.
(30) Garcia-Alloza, M.; Borrelli, L. A.; Rozkalne, A.; Hyman, B. T.; Bacskai, B. J. *J. Neurochem.* **2007**, *102*, 1095.
(31) Yang, F.; Lim, G. P.; Begum, A. N.; Ubeda, O. J.; Simmons, M. R.; Ambegaokar, S. S.; Chen, P. P.; Kayed, R.; Glabe, C. G.; Frautschy, S. A.; Cole, G. M. *J. Biol. Chem.* **2005**, *280*, 5892.
(32) Zhao, Y. W.; Li, J. D.; Wu, Z.; Zhang, H.; Zhao, Y. F.; Yang, R. M.; Lu, L. H. *Microchem. J.* **2021**, *160*.
(33) Wu, Y. Q.; Jing, H.; Dong, Z. S.; Zhao, Q.; Wu, H. Z.; Li, F. Y. *Inorg. Chem.* **2011**, *50*, 7412.
(34) Na, H.; Maity, A.; Teets, T. S. *Dalton Trans.* **2017**, *46*, 5008.
(35) Ma, D. L.; Wong, W. L.; Chung, W. H.; Chan, F. Y.; So, P. K.; Lai, T. S.; Zhou, Z. Y.; Leung, Y. C.; Wong, K. Y. *Angew. Chem., Int. Ed.* **2008**, *47*, 3735.
(36) Ma, X. C.; Jia, J. L.; Cao, R.; Wang, X. B.; Fei, H. *J. Am. Chem. Soc.* **2014**, *136*, 17734.
(37) Cleary, J. P.; Walsh, D. M.; Hofmeister, J. J.; Shankar, G. M.; Kuskowski, M. A.; Selkoe, D. J.; Ashe, K. H. *Nat. Neurosci.* **2005**, *8*, 79.
(38) Benilova, I.; Karran, E.; De Strooper, B. *Nat. Neurosci.* **2012**, *15*, 349.
(39) Brannstrom, K.; Islam, T.; Sandblad, L.; Olofsson, A. *FEBS Lett.* **2017**, *591*, 1167.
(40) Perrin, R. J.; Fagan, A. M.; Holtzman, D. M. *Nature* **2009**, *461*, 916.

TOC Graphic